Highly tolerant tunable waveguide polarization rotator scheme

C. Alonso-Ramos,[1,*] R. Halir,[1] A. Ortega-Moñux,[1] P. Cheben,[2] L. Vivien,[3] Í. Molina-Fernández,[2] D. Marris-Morini,[3] S. Janz,[2] D.-X. Xu,[2] and J. Schmid[2]

[1]*Dpto. Ingeniería de Comunicaciones, ETSI Telecomunicación, Universidad de Málaga, 29010 Málaga, Spain*

[2]*National Research Council of Canada, Ottawa, K1A 0R6, Canada*

[3]*Institut d'Electronique Fondamentale, Univ. Paris-Sud—CNRS UMR8622, Bat. 220, F-91405 ORSAY, France*

**Corresponding author: caar@ic.uma.es*

Received June 15, 2012; accepted July 12, 2012;
posted July 19, 2012 (Doc. ID 170748); published August 21, 2012

Integrated polarization rotators are known to exhibit stringent fabrication tolerances, which severely handicap their practical application. Here we present a general polarization rotator scheme that enables both the compensation of fabrication errors and wavelength tunability. The scheme is described analytically, and a condition for perfect polarization conversion is established. Simulations of a silicon-on-insulator polarization rotator show polarization extinction ratios in excess of 40 dB even in the presence of large fabrication errors that in a conventional rotator configuration degrade the extinction ratio to below 5 dB. Additionally, wavelength tuning over ±30 nm is shown.

OCIS codes: 260.5430, 130.3120, 230.7370.

Polarization management is of fundamental importance in integrated optical devices. The high index contrast of the indium phosphide and silicon-on-insulator platforms enables the design of densely integrated, high-performance devices [1], which exhibit, however, a strong polarization dependence. Polarization diversity approaches are then required [2], for which polarization rotators and splitters are key components. Additionally, in high-speed coherent communication systems, polarization multiplexing is used to enhance transmission efficiency [3], so that integrated transmitter and receiver modules have to provide polarization rotation and polarization splitting/combining functionalities.

For polarization rotation, a large number of implementation alternatives have been described. These include designs based on slanted sidewalls [Fig. 1(a)] as in [4], two-step dry etches [5,6], cross-polarization coupling [7], curved waveguides [8], waveguides with transversal slots [9], and modal evolution [2]. A significant effort has been made to achieve ultrashort devices [10], and conversion lengths of only a few tens of micrometers have been demonstrated using waveguides with longitudinal trenches [Fig. 1(b)]. However, it is well known that polarization rotators exhibit stringent fabrication tolerances [11], which severely limit fabrication yield and thus hinder their application in practical devices. In this Letter, we propose, for the first time, a general polarization rotator scheme that allows for the compensation of fabrication errors. The scheme exploits a combination of phase shifting and polarization rotating waveguide elements, and achieves polarization extinction ratios (ERs) in excess of 40 dB. This remarkable performance is achieved even for large fabrication errors that in a conventional rotator design would degrade the ER to below 5 dB. The resulting device is furthermore wavelength tunable.

The operation of a conventional polarization rotator is illustrated in Fig. 1(c). The device consists of input and output waveguides that support a fundamental horizontally polarized mode (TE) and a fundamental vertically polarized mode (TM), represented with horizontal and vertical arrows in Fig. 1(c). The rotator waveguide between the input and output waveguides supports two orthogonal hybrid modes, $H_{+45°}$ and $H_{-45°}$, polarized at $\theta = 45°$, represented with arrows at $\pm 45°$ in Fig. 1(c). The angle of the polarization axis, θ, is defined as $\theta = \arctan(\iint_\Omega |E_y|^2 d\Omega / \iint_\Omega |E_x|^2 d\Omega)$, with Ω the modal area, and E_x and E_y the horizontal and vertical electrical field components, respectively. The length of the rotator waveguide is the half beat length of the two hybrid modes $L_\pi = \pi/|\beta_{+45°} - \beta_{-45°}|$. Light traveling in the TE polarization of the input waveguides equally excites the two hybrid modes of the rotator waveguide [Fig. 1(c)]. At the end of the rotator waveguides, the hybrid modes have accumulated a π phase shift, so that TM polarized light couples to the output waveguide. Operation with TM polarized input is analogous. Note that the transition between the input and output waveguides and the rotator section can be through direct butt-coupling or a smooth taper to reduce losses [6,10]. The polarization conversion efficiency (PCE), i.e., the percentage of power transferred from a given input polarization to the orthogonal

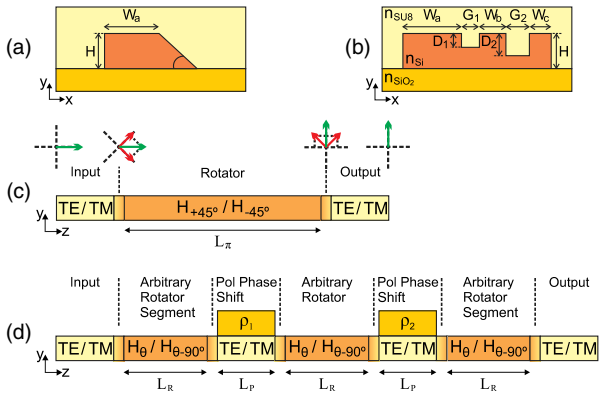

Fig. 1. (Color online) (a) Cross section of a slanted rotator waveguide and (b) a rotator waveguide with longitudinal trenches. (c) Schematic of a conventional polarization rotator. (d) Schematic of the proposed polarization rotator scheme.

output polarization, is given by $\mathrm{PCE} = \sin^2(2\theta)\sin^2(\frac{\pi}{2}L_R/L_\pi)$, where L_R is the physical length of the rotator waveguide [4]. From this expression it is obvious that the PCE of a conventional rotator is highly sensitive to variations in the polarization axis angle, θ, and the beat length of the hybrid modes, L_π, both of which strongly depend on the waveguide geometry. Even small fabrication imperfections can thus substantially degrade the performance of the rotator [11].

To solve the tolerance sensitivity problem, we propose a new polarization rotator scheme, as shown schematically in Fig. 1(d). The rotator scheme consists of an input and output waveguide supporting both fundamental TE and TM modes, three rotator segments (RSs) with a polarization axis angle θ, and two tunable polarization phase shifters (PPSs) that introduce a phase delay ρ_i between the fundamental TE and TM modes. The concept that underlies this approach is the following. The three RSs are realized with waveguides that produce a polarization axis angle θ, which may deviate significantly from the nominal 45° angle. This deviation is compensated by the tunable polarization phase delays ρ_1 and ρ_2, which can be implemented, for example, with waveguide heaters or carrier injection in a p-i-n waveguide diode.

The behavior of each RS can be described via the Jones matrix $\mathbf{R} = \mathbf{A}(\theta)\cdot\mathbf{D}(\phi)\cdot\mathbf{A}(-\theta)$, where

$$\mathbf{A}(\theta) = \begin{pmatrix} \cos\theta & -\sin\theta \\ \sin\theta & \cos\theta \end{pmatrix}, \qquad \mathbf{D}(\phi) = \begin{pmatrix} \exp(j\phi) & 0 \\ 0 & 1 \end{pmatrix}, \tag{1}$$

and $\phi = |\beta_\theta - \beta_{\theta-90°}|L_R$, with β_θ and $\beta_{\theta-90°}$ the propagation constants of the hybrid modes and L_R the physical length of the rotator waveguide. The PPSs are modeled as $\mathbf{D}(\rho_i)$, with $\mathbf{D}$ as defined in Eq. (1) and $\rho_i = (\beta_{\mathrm{TE}} - \beta_{\mathrm{TM}})L_P$, where L_P is the physical length of the PPS waveguide. The Jones matrix of the complete polarization rotator scheme is thus $\mathbf{R}\cdot\mathbf{D}(\rho_2)\cdot\mathbf{R}\cdot\mathbf{D}(\rho_1)\cdot\mathbf{R}$, from which after some algebra the following analytical condition for perfect polarization conversion is obtained:

$$\sin^2(2\theta)\sin^2(\phi/2) > \frac{1}{4}. \tag{2}$$

This tolerance condition, which is one of the main results of this paper, establishes the tolerance limits for the rotator waveguide so that perfect polarization conversion is possible with compensatory polarization phase shifts ρ_1 and ρ_2. Condition (2) is plotted in Fig. 2(a), showing that perfect rotation is feasible for polarization axis angles as small as $\theta = 15° - 20°$ for a comparatively large phase range $\phi \sim 100° - 180°$, the latter indicating a good tolerance for the rotator waveguide length. By way of example, Fig. 2(b) shows a Poincaré sphere representation of the transition from TE to TM polarization using rotators with $\theta = 20°$, $\phi = 110°$ and $\rho_1 = 132.2°$, $\rho_2 = 58.8°$. In a conventional rotator design, such a large axis angle deviation from $\theta = 45°$ actually yields more power in the TE mode than in the TM mode.

Three RSs and two PPSs are the minimum number of elements required to achieve perfect polarization rotation with imperfect RS. Increasing the number of elements will result in more external controls for the tuning elements, and reduced bandwidth as discussed below.

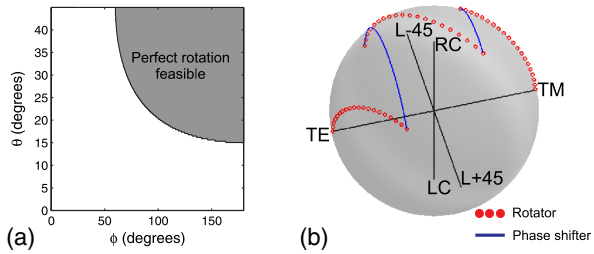

Fig. 2. (Color online) (a) Graphical representation of condition (2) for perfect polarization rotation; (b) Poincaré-sphere plot of a perfect rotation with a polarization axis at $\theta = 20°$ using our rotator scheme.

As an example of high efficiency of our polarization rotator scheme, we implement it in a silicon-on-insulator rotator based on the design by Velasco *et al.* [10]. The waveguides are $H = 260$ nm high and $W = 415$ nm wide, and are covered with SU8. The refractive indices of the bottom oxide, silicon waveguide core, and SU8 cladding at $\lambda = 1.55$ μm are $n_{\mathrm{SiO_2}} = 1.444$, $n_{\mathrm{Si}} = 3.476$, and $n_{\mathrm{SU8}} = 1.58$, respectively. The corresponding thermo-optical coefficients are $dn_{\mathrm{SiO_2}}/dT = 1\times10^{-5}\,°\mathrm{C}^{-1}$, $dn_{\mathrm{Si}}/dT = 1.8\times10^{-4}\,°\mathrm{C}^{-1}$, and $dn_{\mathrm{SU8}}/dT = -1.1\times10^{-4}\,°\mathrm{C}^{-1}$ [12,13]. The cross section of the rotator waveguide used in [10] is shown in Fig. 1(b). The trenches of different depths are defined using the calibrated etch-lag effect. The nominal dimensions of the gaps are $G_1 = 60$ nm and $G_2 = 85$ nm, which are etched to depths $D_1 = 210$ nm and $D_2 = 238$ nm, and are separated by widths $W_a = 200$ nm, $W_b = 40$ nm, and $W_c = 30$ nm. All results shown in the following correspond to three-dimensional (3D), full-vectorial simulations of the complete rotator structure, using the commercial Fimmwave package.

In the conventional rotator scheme [Fig. 1(c)], the rotator waveguide is 13 μm long and is connected to the input and output with low loss transitions. The simulated ER of this device, defined as $\mathrm{ER[dB]} = 10\log_{10}(P_{\mathrm{TM,out}}/P_{\mathrm{TE,out}})$ when TE polarized light is launched into the device, exceeds 25 dB when all device dimensions are nominal. However, as shown in Fig. 3, variations of 5% in the size of the trenches can reduce the ER to

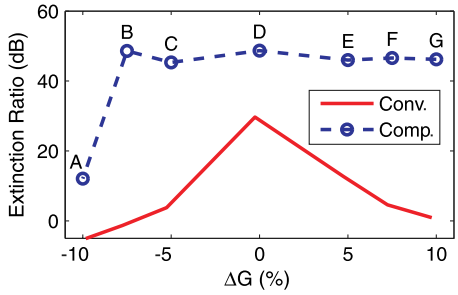

Fig. 3. (Color online) ER of a conventional rotator and the proposed rotator scheme for various fabrication variations at $\lambda = 1.55$ μm. Temperatures increments $(\Delta T_1, \Delta T_2)$ to achieve compensation are A, (16.5 °C, 16.1 °C); B, (25.9 °C, 10.4 °C); C, (31 °C, 9.3 °C); D, (33.2 °C, 8.7 °C); E, (12.3 °C, 37.1 °C); F, (2.6 °C, 17.2 °C); G, (19.8 °C, 2.1 °C).

Table 1. ER for Different Operational Wavelengths in a Conventional Rotator (ER conv.) and in Our Approach (ER comp.) with $\Delta G = +5\%$

λ	ER Conv.	ER Comp.	ΔT_1	ΔT_2
1.52 μm	10.9 dB	46.3 dB	38.1 °C	12.1 °C
1.58 μm	10.3 dB	46.5 dB	25 °C	36.8 °C

below 5 dB. Similar performance deteriorations are generally observed in other rotators, severely limiting their application in practical devices.

The rotator scheme we propose can compensate for the largest deviation in polarization axis angle (θ) when the length of the RS (L_R) is such that $\phi = |\beta_\theta - \beta_{\theta-90°}|L_R = 180°$ [Fig. 2(a)]. We thus set L_R to the nominal value $L_R = \pi/|\beta_{+45°} - \beta_{-45°}| \sim 13$ μm.

Planar waveguides generally exhibit an appreciable polarization dependence [14,15], which can be exploited to obtain PPS [16]. By way of example, here we use the thermo-optic effect of the interconnecting waveguide for polarization phase shifting. In these waveguides the TE mode is mainly confined within the silicon waveguide core, which has a positive thermo-optical coefficient. Hence, its effective index appreciably increases with temperature; the simulated rate is $dn_{\mathrm{eff,TM}}/dT = 1.7 \times 10^{-4}\ °\mathrm{C}^{-1}$. The TM mode strongly senses the SU8 cladding, which has a negative thermo-optical coefficient, thus reducing the rate to $dn_{\mathrm{eff,TM}}/dT = 1.1 \times 10^{-4}\ °\mathrm{C}^{-1}$. The temperature dependent polarization phase shift is then given by $\rho = L_P \frac{2\pi}{\lambda}(n_{\mathrm{eff,TE}} - n_{\mathrm{eff,TM}}) + L_P \frac{2\pi}{\lambda}(dn_{\mathrm{eff,TE}}/dT - dn_{\mathrm{eff,TM}}/dT)\Delta T$. There is a tradeoff in choosing the length of the PPS (L_P): longer PPSs require lower temperature increments, but are also increasingly narrowband, and constitute the main bandwidth limitation of this scheme. We set $L_P = 700$ μm so that ρ can be varied over 360° with temperature increments $\Delta T < 40\ °\mathrm{C}$, while ensuring an ER in excess of 30 dB over a 0.8 nm DWDM channel. By spiralling the shifter waveguide, a compact footprint and lower power consumption can be achieved [13].

Figure 3 shows that the rotator scheme we propose can fully compensate fabrication variations between $\Delta G = -7.5\%$ and $\Delta G = +10\%$, with ER in excess of 40 dB. The temperatures increments (ΔT_1, ΔT_2) in the PPS required for compensation are shown in the caption of Fig. 3 and can be found through iteration or using an optimization algorithm. For $\Delta G = -10\%$ (point A) the rotator waveguide parameters are $\theta = 15.5°$ and $\phi = 74°$, and thus lay outside the region that can be fully compensated [Fig. 2(a)]. However the ER is still improved compared to the conventional design.

Our scheme furthermore allows for retuning of the device to an arbitrary wavelength, as long as Eq. (2) holds for this wavelength. Table 1 shows the waveguide temperatures required to tune the device to $\lambda = 1.52$ μm and $\lambda = 1.58$ μm, achieving ER in excess of 40 dB, even in the presence of fabrication errors of $\Delta G = +5\%$.

We have proposed a general tuning scheme for polarization rotators that provides highly tolerant, wavelength tunable devices. This scheme can efficiently compensate errors arising from fabrication imperfections, and only requires PSSs that can be realized with simple waveguide heaters. This polarization rotator scheme thus overcomes the practical limitations of existing rotator designs, thereby enabling their use for polarization diversity and polarization multiplexing in integrated optical circuits.

References

1. R. Halir, G. Roelkens, A. Ortega-Moñux, and J. G. Wangüemert-Pérez, Opt. Lett. **36**, 178 (2011).
2. T. Barwicz, M. Watts, M. Popovic, P. Rakich, L. Socci, F. Kärtner, E. Ippen, and H. Smith, Nat. Photon. **1**, 57 (2007).
3. E. Ip, A. Lau, D. Barros, and J. Kahn, Opt. Express **16**, 753 (2008).
4. H. Deng, D. Yevick, C. Brooks, and P. Jessop, J. Lightwave Technol. **23**, 432 (2005).
5. D. Vermeulen, S. Selvaraja, P. Verheyen, W. Bogaerts, D. Van Thourhout, and G. Roelkens, in *Group IV Photonics* (IEEE, 2010), p. 42.
6. C. Alonso-Ramos, S. Romero-García, A. Ortega-Moñux, I. Molina-Fernández, R. Zhang, H. Bach, and M. Schell, Opt. Lett. **37**, 335 (2012).
7. L. Liu, Y. Ding, K. Yvind, and J. M. Hvam, Opt. Lett. **36**, 1059 (2011).
8. D. Dai and J. E. Bowers, Opt. Express **19**, 10940 (2011).
9. M. Kotlyar, L. Bolla, M. Midrio, L. O'Faolain, and T. Krauss, Opt. Express **13**, 5040 (2005).
10. A. Velasco, M. L. Calvo, P. Cheben, A. Ortega-Moñux, J. H. Schmid, C. Ramos, Í. M. Fernandez, J. Lapointe, M. Vachon, S. Janz, and D.-X. Xu, Opt. Lett. **37**, 365 (2012).
11. H. Deng, D. Yevick, C. Brooks, and P. Jessop, J. Opt. Soc. Am. A **23**, 1741 (2006).
12. J. Schmid, M. Ibrahim, P. Cheben, J. Lapointe, S. Janz, P. Bock, A. Densmore, B. Lamontagne, R. Ma, W. Ye, and D.-X. Xu, Opt. Lett. **36**, 2110 (2011).
13. A. Densmore, S. Janz, R. Ma, J. Schmid, D.-X. Xu, A. Delâge, J. Lapointe, M. Vachon, and P. Cheben, Opt. Express **17**, 10457 (2009).
14. Y. Inoue, K. Katoh, and M. Kawachi, IEEE Photon. Technol. Lett. **4**, 36 (1992).
15. J. van der Tol, L. Augustin, U. Khalique, and M. Smit, in *Proceedings of 13th Micro Optic Conference* (IEEE, 2007), p. C1.
16. J.-W. Kim, S.-H. Park, W.-S. Chu, and M.-C. Oh, Opt. Express **20**, 12443 (2012).